

THE EFFECT OF OXIDATION IN ENVIRONMENTAL BARRIER COATINGS SUBJECT TO FOREIGN OBJECT DAMAGE

Leland C. Hoffman
HX5, LLC.
Brook Park, OH

Michael J. Presby, Jamesa L. Stokes, Bryan J. Harder, Jonathan A. Salem
NASA Glenn Research Center
Cleveland, OH

ABSTRACT

Oxidation and foreign object damage (FOD) are two key failure modes for environmental barrier coatings (EBCs). For EBCs with a silicon (Si) bond coat, a thermally grown oxide (TGO) layer forms at the EBC – bond coat interface. The TGO layer is considered the weak interface, and directly influences the life of the EBC. Moreover, FOD has been shown to cause significant subsurface damage resulting in delamination or spallation of the EBC which can occur at the EBC - bond coat interface or the bond coat - substrate interface. The purpose of this work is to investigate the synergistic effects of oxidation and FOD in a ytterbium disilicate ($Yb_2Si_2O_7$) EBC. FOD testing is conducted on as-deposited and steam oxidized samples at room temperature using a 1.59 mm hardened steel ball projectile. The resulting damage is characterized by optical profilometry and scanning electron microscopy (SEM). Additionally, a quasi-static, mechanical assessment of the EBC bond strength in the presence of a growing TGO is presented.

Keywords: environmental barrier coatings (EBCs), silicon carbide (SiC), foreign object damage (FOD), oxidation, impact, thermally grown oxide (TGO)

1. INTRODUCTION

Silicon carbide (SiC) based ceramic matrix composites (CMCs) are considered enabling materials for gas turbine engines due to their higher temperature capability and low density. These properties allow for higher material operating temperatures that can lead to improved engine efficiency and reduced emissions due to lower cooling requirements. Despite these beneficial properties at high temperature, the protective

silica (SiO_2) scale responsible for oxidation resistance reacts with water vapor to form a volatile silicon hydroxide ($Si(OH)_4$), which in turn causes surface recession [1-5]. To combat these reactions, environmental barrier coatings (EBCs) have been developed. Current generation EBCs, developed for 1,316°C (2,400°F) capable CMCs, are based on rare-earth (RE) silicates with the general formulas RE_2SiO_5 (RE monosilicate) and $RE_2Si_2O_7$ (RE disilicate). Candidate RE elements are yttrium, ytterbium, scandium, or lutetium [6]. In addition, silicon (Si) is incorporated as a bond coat to provide suitable adhesion and acts as another barrier to oxidation of the underlying CMC substrate.

A key life-limiting failure mechanism for EBC/CMC systems is oxidation. Under combustion conditions, the rate of oxidation of Si-based materials is an order of magnitude faster than in dry oxygen. The scale growth is parabolic in nature and has been extensively studied in literature [7-8]. Under an EBC, the SiO_2 thermally grown oxide (TGO) forms at the EBC/Si bond coat interface, and the growth rate remains parabolic. Understanding the effect of the TGO on the durability and life of the EBC is of great importance. A previous study, performed on an EBC (ytterbium disilicate) applied directly to a SiC substrate without an Si bond coat, showed the adhesion strength of an EBC was critically reduced in the presence of a TGO layer and that failure preferentially occurred at the TGO interface [9].

In addition to oxidation, foreign object damage (FOD) is a key failure mode of interest in EBC/CMC systems [10-15]. A large variety of foreign objects can be ingested into the engine including, but not limited to, ice, salt, sand, as well as birds and runway debris. Objects within the engine such as spalled coating material and metallic debris have also been observed to cause

This manuscript is a joint work of employees of the National Aeronautics and Space Administration and employees of HX5, LLC. under Contract No. 80GRC020D0003 with the National Aeronautics and Space Administration. The United States Government may prepare derivative works, publish, or reproduce this manuscript and allow others to do so. Any publisher accepting this manuscript for publication acknowledges that the United States Government retains a non-exclusive, irrevocable, worldwide license to prepare derivative works, publish, or reproduce the published form of this manuscript, or allow others to do so, for United States government purposes.

downstream damage [10]. While FOD has been widely investigated for metallic gas turbine materials, monolithic ceramics, and CMCs, there have been very limited studies on the effect of FOD in EBCs. FOD can cause cracking, delamination, or spallation of the EBC leading to the ingress of combustion gases to the CMC substrate that can result in rapid material degradation.

The present study was conducted to understand the synergistic effects of steam oxidation and FOD on NASA's second generation EBC, ytterbium disilicate ($\text{Yb}_2\text{Si}_2\text{O}_7$), with an Si bond coat. A quasi-static, mechanical assessment of the EBC bond/adhesion strength with varying thickness of TGO layer is presented along with a qualitative comparison to the FOD morphology.

2. MATERIALS AND METHODS

2.1 Target Materials

The substrates used in this study were Hexoloy SA (Saint Gobain) monolithic silicon carbide (SiC). Monolithic SiC is used for several reasons: (1) monolithic SiC is often used as a surrogate substrate for EBC development [16-18], (2) previous FOD studies on EBCs have used monolithic SiC substrates [13, 19], and (3) the relative high cost, and limited availability of CMC substrates. Future work will expand upon these initial findings by depositing the same EBC system on CMC substrates.

The substrates used for FOD were 25.4 x 12.7 x 3.2 mm while those used for the mechanical assessment of the EBC adhesion strength were 25.4 mm diameter by 3mm thick. For all samples, the SiC substrate was first grit blasted with cubic boron nitride prior to the deposition of a nominally 127 μm (5 mil) thick Si bond coat, and a 254 μm (10 mil) thick $\text{Yb}_2\text{Si}_2\text{O}_7$ EBC. The Si bond coat and EBC were both deposited via an air plasma spray process by Curtiss Wright (East Windsor, CT).

2.2 Steam Exposure

Samples were exposed in a flowing steam environment at 1,316°C. The steam furnace configuration has been described in detail in other publications [5,20], but is discussed here briefly. Samples were suspended in a platinum basket in a vertical tube furnace with steam (90% $\text{H}_2\text{O}/\text{O}_2$) flowing at 13 cm/s. The FOD samples were cyclically exposed at one-hour intervals for 100, 200, and 300 hours, while the samples used for adhesion strength underwent an isothermal exposure (no cycling) for 60, 150, and 300 hours. Witness coupons were cross-sectioned, polished to a 1 μm finish, and analyzed using a Phenom ProX desktop Scanning Electron Microscope (SEM) to determine the corresponding TGO thickness.

2.3 Adhesion Strength Testing

The adhesion strength of the EBC was determined using a traditional "pull-test" method used to determine the through-thickness tensile strength. Additionally, this test method is expected to provide information regarding the location of the weak interface in this material system. This method was used in a other publications [9,21] where a more detailed description can

be found. The traditional pull test method was performed in accordance with ASTM D7291-15 [22] with some deviations. Ti-6Al-4V pull tabs were machined and bonded to the sample; one to the EBC and one to the substrate, using Solvay FM1000 adhesive. The pull tabs were undersized (85%) compared to the 25.4 mm sample in order to minimize edge effects. A servohydraulic MTS test frame fitted with a 100 kN load cell was used to load the samples in displacement control mode at a rate of 0.002 mm/s. The EBC adhesion strength was recorded as the peak stress during each test. At least two samples were tested at each steam exposure durations of 0, 60, 150, and 300 hours.

2.4 Foreign Object Damage Testing

Impact testing was performed using a gas gun to accelerate a hardened 1.59 mm chrome steel ball (HRC 60) projectile. A reservoir was filled with helium to the required pressure and a fast-acting solenoid valve subsequently opened, accelerating the spherical projectile down the barrel. Two holes near the end of the barrel facilitated the use of a dual laser gate system, monitored by a Keysight model DSOX 1204A digital oscilloscope, to determine the projectile velocity. The sample was positioned 50 mm from the end of the barrel (110 mm from the laser gate) and it was assumed that there was negligible change in velocity over this distance. All samples were mounted at a normal incidence angle in a fully supported configuration on a stainless-steel backing plate [11]. FOD testing was performed on as-deposited (non-oxidized) as well as steam-oxidized samples. Three as-deposited EBC samples were impacted at each of the following projectile velocities: 50, 75, 100, 125, 150, 175, 200, and 300 m/s. Two samples each were tested at 50, 75, and 100 m/s for each of the 100, 200, and 300 hour steam exposures. The post-impact damage was first characterized using a 3200 series Keyence Profilometer to understand the extent of the surface damage.

2.5 Hardness Testing

Hardness testing was performed on the as-deposited EBC as well as the 100, 200, and 300 hour steam cycled EBCs. The EBC surfaces were polished to a 1 μm finish to better facilitate measurement of the indent size. A Struers Durascan 70 was used to perform the 49 N Vicker's hardness tests. A series of six indents were made on each sample.

3. RESULTS AND DISCUSSION

3.1 Material Composition and Characterization

The coating hardness (Fig. 1) was observed to increase after steam exposure. The baseline EBC had the lowest hardness of 4.8 ± 0.17 GPa and the 300 hour steam exposed sample had the highest at 7.3 ± 0.57 GPa; however, the majority of the change in hardness had already occurred by 100 hours of steam exposure. Coating densification and other microstructural changes such as crystallization occurring during the steam exposure was assumed to be the cause of the increased hardness. Additionally, changes in mechanical properties could be caused by the formation of monosilicate. An attempt was made to determine the indentation

fracture toughness for the as-deposited and steam oxidized samples, although the cracks emanating from the corners of the indent generally interacted with porosity or experienced significant crack bifurcation/branching. Further efforts to understand the mechanical properties of the as deposited and steam oxidized EBC are warranted as will be discussed more in later sections.

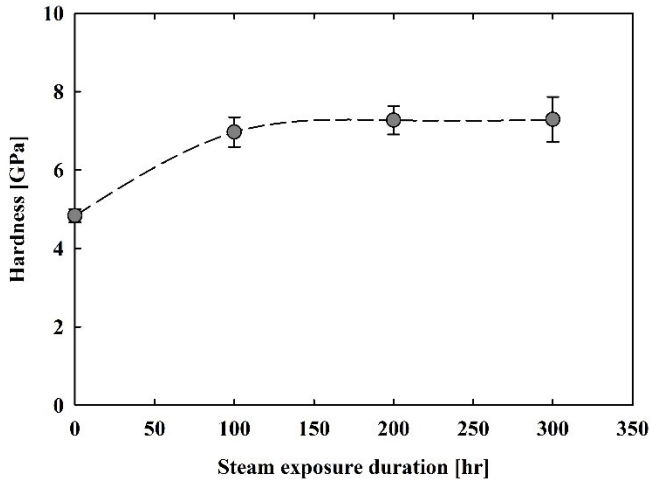


FIGURE 1: EBC HARDNESS AS A FUNCTION OF STEAM EXPOSURE DURATION. TRENDLINES ADDED FOR CLARITY.

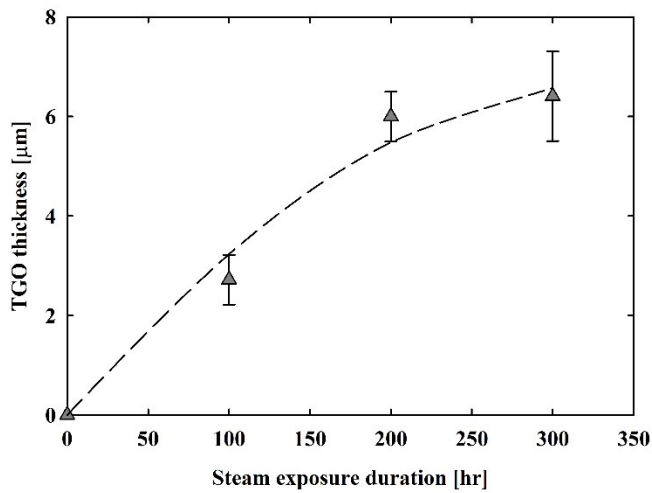


FIGURE 2: TGO THICKNESS AS A FUNCTION OF STEAM EXPOSURE DURATION.

Fig. 2 shows the measured TGO thickness as a function of steam exposure duration. The TGO was measured to be $2.7 \pm 0.5 \mu\text{m}$ after 100 hours of steam cycling and increased to $6.4 \pm 0.9 \mu\text{m}$ after 300 hours. Representative images of the as deposited and steam oxidized samples are shown in Fig. 3 where the TGO is observed at the EBC – Si bond coat interface.

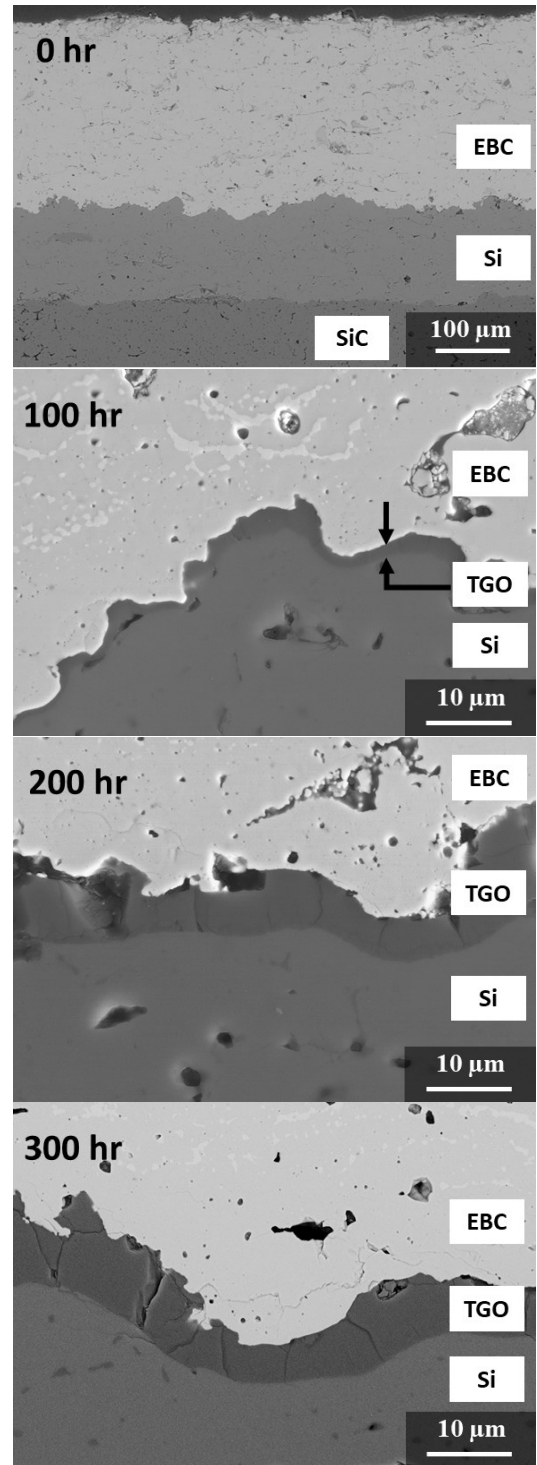


FIGURE 3: REPRESENTATIVE SEM IMAGES OF THE AS-DEPOSITED EBC AND THE SiO_2 TGO GROWTH AFTER 100, 200, AND 300 HOURS OF STEAM EXPOSURE.

3.2 Steam Oxidized EBC Adhesion Strength

The adhesion strength was recorded as the maximum stress obtained during each test. Typical steam exposed samples exhibited catastrophic failure at all durations with failures becoming more brittle as the steam exposure time increased. Representative images of the 0, 60, and 300 hour samples are shown in Fig. 4. Failure occurred in the TGO layer with some pullout of the Si bond coat. In all steam-exposed samples, failure initiated in the TGO layer and propagated through the TGO and along the TGO – Si bond coat interface, although some evidence of crack propagation along the TGO – EBC interface was also observed. Regardless, failure always occurred within or along one of the interfaces of the TGO. The as-deposited samples, on the other hand, typically failed at the Si bond coat – SiC substrate interface. The adhesion strength plotted as a function of steam exposure is shown in Fig. 5 and shows that the adhesion strength of the EBC decreases as steam exposure, and correspondingly TGO thickness, increases. The 300 hour steam exposed samples have about 56% the adhesion strength of the samples exposed for 60 hours.

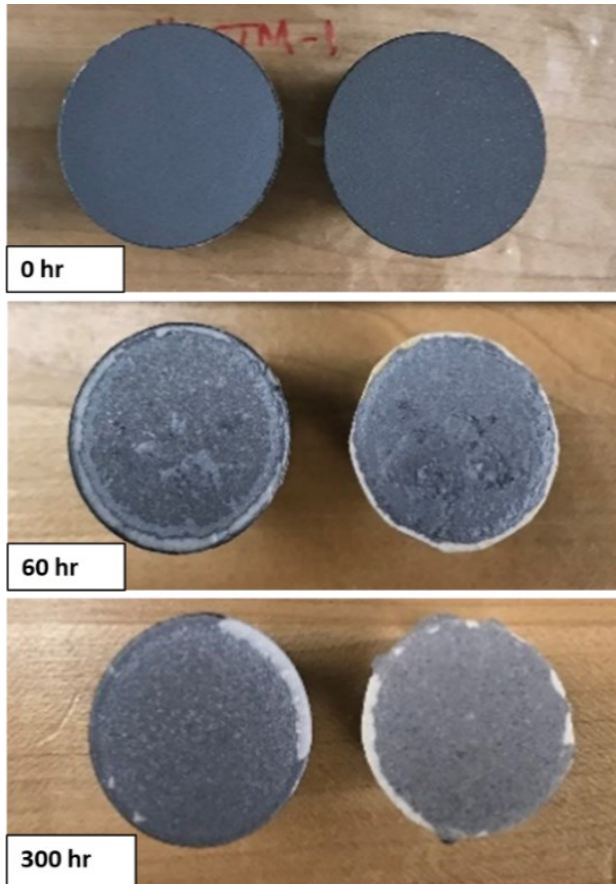


FIGURE 4: REPRESENTATIVE IMAGE SHOWING FAILURE OF 0, 60, AND 300 HOUR STEAM EXPOSED SAMPLES SUBJECT TO ADHESION STRENGTH TESTING (25.4 MM COUPON).

It is noted that the as-deposited samples had very poor bond strength and failure generally occurred at the Si bond coat – SiC substrate interface. It is speculated that the poor adhesion is due to residual stresses within the EBC and Si bond coat from the deposition processes, and that the steam exposure may have an annealing effect which relieves residual stresses and increases the adhesion of the bond coat to the substrate. Current investigations are underway to determine the cause of the lower bond strength observed in the as-deposited samples. Nonetheless, as the TGO layer increases during steam exposure, the adhesion strength is reduced, and the TGO appears to be the preferential location for failure (e.g., the weak interface).

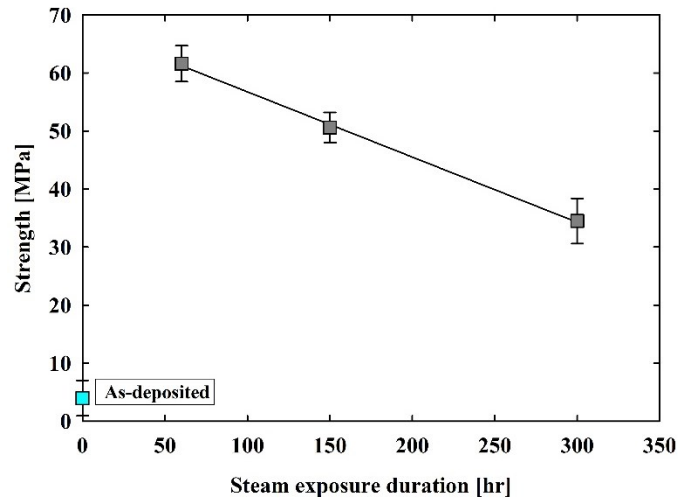


FIGURE 5: STRENGTH OF STEAM EXPOSED AND AS-PROCESSED SAMPLES.

3.3 As-deposited Impact Damage

From the profilometry data, the impact crater depth (Fig. 6) and diameter (Fig. 7) were plotted as a function of projectile velocity. The crater diameter and depth follow a similar increasing trend with increasing impact velocity. At velocities lower than 150 m/s, the prevailing external damage was a simple crater with material protrusion and ejection around the perimeter of the crater as shown in Fig. 8. Above 150 m/s, the damaged zone reached the depth of the Si bond coat resulting in spallation of the EBC along the Si bond coat interface. At 200 m/s, half of the samples experienced catastrophic failure of the substrate, as did all samples tested above 200 m/s.

While profilometry is useful in determining the magnitude of external surface damage, SEM images of sample cross-sections were taken to form a more complete characterization of the internal or sub-surface damage. To analyze the internal damage, samples impacted at 50, 100, 150, and 200 m/s were sectioned along the long transverse plane at the mid-plane of the impact site. Representative images of the internal damage at various impact velocities can be seen in Fig. 9. It was seen that delamination occurred preferentially at the interface of the Si bond coat and SiC substrate, indicating that bond coat adhesion

was the limiting factor for delamination in the as-deposited samples. At velocities less than 75 m/s, EBC crushing, micro-cracking, and cone cracking that propagated into the bond coat were observed. At intermediate velocities (100-150 m/s) more severe EBC deformation occurred through crushing and perimetral protrusion and ejection. Large transverse and radial cracks propagated through the EBC and cone cracking extended down through the bond coat. At velocities of 175-200 m/s, significant spallation of the EBC was observed. It is hypothesized that as the impact velocity increases, the cracks seen at intermediate velocities extend to and subsequently travel along the EBC - Si bond coat interface, resulting in spallation. At all velocities, delamination at the Si bond coat – SiC substrate interface was also observed. At and above 200 m/s complete fracture of the SiC substrate occurred.

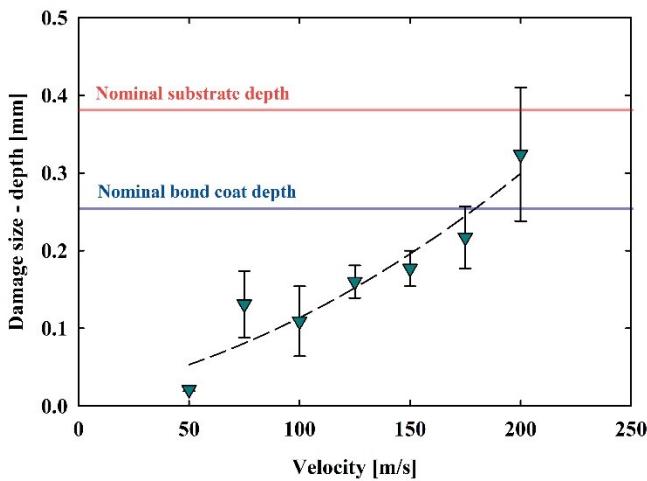


FIGURE 6: DEPTH OF IMPACTED REGION VERSUS IMPACT VELOCITY. THE NOMINAL BOND COAT AND SUBSTRATE DEPTHS ARE SHOWN FOR COMPARISON.

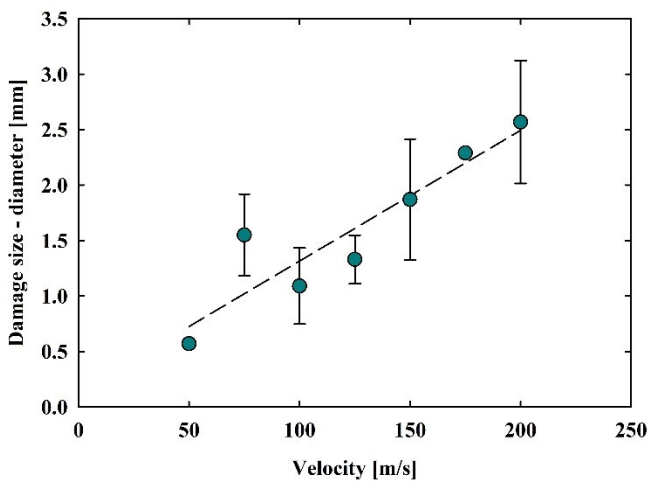


FIGURE 7: DIAMETER OF IMPACTED DAMAGE VERSUS IMPACT VELOCITY.

The delamination length at the Si bond coat – SiC substrate interface was measured and increased with impact velocity up to 150 m/s, at which point complete delamination along the length of sample was observed as shown in Fig. 8. A previous FOD study performed on hot-section metallic vane airfoils with a columnar thermal barrier coating (TBC) deposited by electron beam, physical vapor deposition (EB-PVD) [12] showed that delamination in that system primarily occurred at the TBC topcoat and platinum aluminide (PtAl) bond coat interface, or along the TGO interface that exists between the TBC topcoat and PtAl bond coat. For comparison, the delamination data observed the TBC system [12] has been plotted along with that of the present work. There are two important differences when comparing the results of these two studies. First, the delamination in the EBC/Si/SiC system is primarily observed to occur at the Si bond coat – SiC substrate interface while the delamination in the TBC/PtAl superalloy system primarily occurred at the TBC/PtAl bond coat interface. Second, the measured delamination length in the TBC system is much smaller suggesting the TBC system has better FOD and delamination resistance.

These are two critical observations that need to be considered in understanding the difference in FOD damage morphology and for designing more FOD resistant EBCs. It should be noted that future work is warranted for EBCs deposited on CMC substrates to generate a more complete understanding of FOD for these materials.

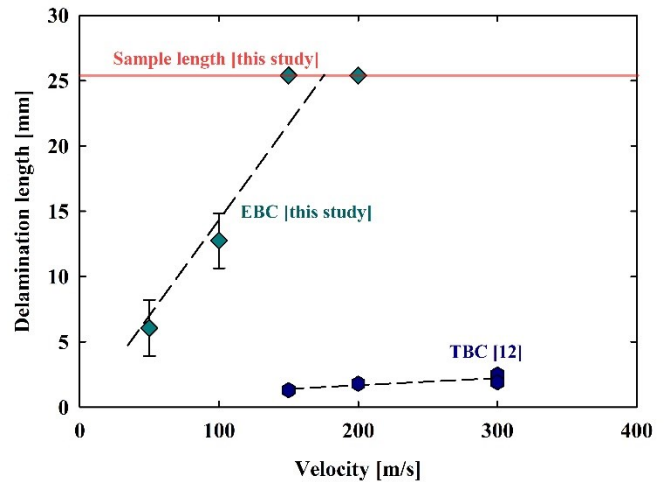


FIGURE 8: DELAMINATION LENGTH FROM THE AS-DEPOSITED EBCS IMPACTED IN THE PRESENT STUDY AS WELL AS PREVIOUS DATA FROM THERMAL BARRIER COATINGS (TBC) DEPOSITED ON HOT-SECTION VANE AIRFOILS [12].

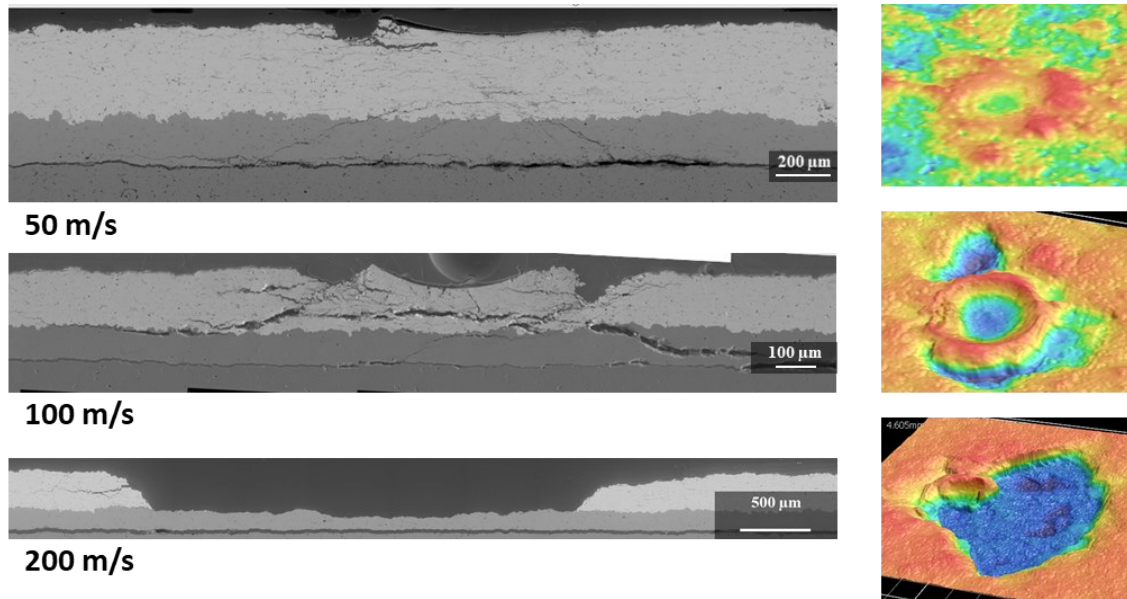


FIGURE 9: REPRESENTATIVE SEM AND PROFILOMETRY IMAGES OF SAMPLES IMPACTED AT 50 (TOP), 100 (MIDDLE), AND 200 M/S (BOTTOM).

3.4 Impact Damage of Oxidized Samples

Two samples each were tested at 50, 75, and 100 m/s for each of the 100, 200, and 300 hour steam exposure scenarios. External/surface damage of these samples was very limited. There was no evidence of EBC crushing, protrusion, or ejection as was observed in the as-deposited samples. Crater depths and widths were minimal and could not easily be measured as the crater dimensions fell within the typical peaks and valleys of the surface roughness of the topcoat. The increased hardness and densification of the EBC after steam exposure are believed to be two of the contributing factors for the lack of external damage/crater formation as these material changes would increase resistance to projectile penetration. It appeared that the as-deposited EBC was more compliant while the steam oxidized EBC was much more rigid. In addition, the critical velocity for substrate fracture to occur at all steam exposure durations was 100 m/s, compared to 200 m/s for the as-deposited samples. It appeared that the as-deposited EBC was able to dissipate more impact energy through crushing and crack formation while the oxidized EBC was much more rigid. This underscores that there is a limiting substrate effect when using monolithic SiC. It is currently assumed that the FOD damage morphology at velocities lower than the critical impact velocity is still representative, but as mentioned previously, future work on CMC substrates will be critical to a more complete understanding of FOD in EBCs.

In the same manner as the as-deposited samples, the steam exposed samples were sectioned, polished, and inspected under SEM. Internal damage was localized to only the immediate vicinity of the impact site. Even at the highest survivable velocities, widespread delamination and cracking were not present. At 75 m/s, the upper limit before substrate failure, there was radial and transverse cracking in the EBC at the impact site,

but not to the extent observed in the as-deposited samples. Localized delamination that occurred along the TGO interface was on the order of 2 ± 1 mm and was observed only for the samples impacted at 75 m/s (Fig. 10). At this velocity some samples experienced hairline cracks in the substrate but did not fully fracture. In general, the impact damage was more brittle and showed little to no EBC deformation in the form of a quantifiable impact crater. There was no notable increase in surface or subsurface damage with longer steam exposure. For example, samples exposed to 100 hours of steam incurred similar damage as those exposed for 300 hours when impacted at the same velocity.

The increased hardness and densification of the EBC after steam exposure are also believed to be contributing factors to the reduced subsurface damage observed in the steam-oxidized samples. Additionally, the relationship between quasi-static material properties and the dynamic material behavior of the EBC system upon impact is not currently known. Moreover, significant delamination was observed in the as-deposited samples, but the extent of delamination was significantly reduced in the steam oxidized samples. It was hypothesized, based on the quasi-static mechanical assessment of the adhesion strength, that delamination would readily occur along the TGO interface; however, this was not the case and any trend based on impact velocity and steam exposure could not be generated.

Ultimately, the observations of this work highlight the complexity in understanding the synergistic effects of different degradation modes in EBCs. A better understanding of the effect of steam exposure on the mechanical properties of the EBC is required. Additionally, any difference in material properties and response under quasi-static and dynamic loading conditions should be further investigated. Combined experimental and computational approaches should also be leveraged.

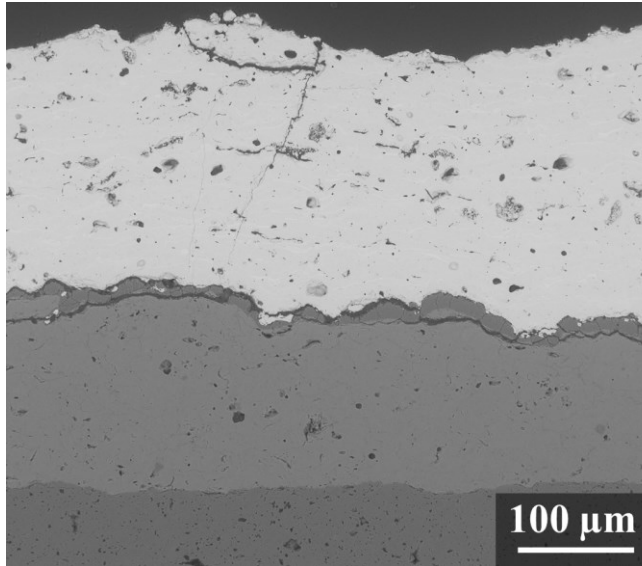


FIGURE 10: SEM OF A 200 HOUR STEAM-EXPOSED SAMPLE IMPACTED AT 75 M/S SHOWING TGO DELAMINATION.

4. CONCLUSION

- TGO growth was shown to considerably reduce the adhesion strength of an EBC, with failure preferentially occurring at the TGO layer
- FOD in as-deposited samples resulted in EBC crushing, protrusion, and ejection as well as widespread delamination at the bond coat - substrate interface.
- FOD in steam-oxidized samples resulted in more brittle damage mechanisms and had a critical substrate fracture velocity (100 m/s) that was half that of the as-deposited samples (200 m/s).

ACKNOWLEDGEMENTS

This work was supported by the NASA Aeronautics Research Mission Directorate (ARMD) Transformational Tools and Technologies (TTT) Project. The authors would like to thank Jeffrey Hammel, Pete Bonacuse, Chris Burke and Drew Davidson for their valuable assistance in fabrication, testing, and post-test analysis.

REFERENCES

[1] J. Smialek, C. Robinson, E. Opila, D. Fox, and N. Jacobson, SiC and Si₃N₄ Recession Due to SiO₂ Scale Volatility Under Combustor Conditions, *Adv. Compos. Mater.*, 8(1), 1999, 33–45.

[2] E. Opila, J. Smialek, C. Robinson, D. Fox, and N. Jacobson, SiC Recession Caused by SiO₂ Scale Volatility Under Combustion Conditions: II, Thermodynamics and Gaseous-Diffusion Model, *J. Am. Ceram. Soc.*, 82(7), 1999, 1826–1834.

[3] N. Jacobson, Corrosion of Silicon-Based Ceramics in Combustion Environments, *J. Am. Ceram. Soc.*, 76(1), 1993, 3–28.

[4] N. Jacobson, D. Fox, J. Smialek, E. Opila, C. Robinson, *Performance of Ceramics in Severe Environments*, 2005, 1-14.

[5] K. Lee, D. Fox, J. Eldridge, D. Zhu, C. Robinson, N. Bansal, and R. Miller, Upper Temperature Limit of Environmental Barrier Coatings Based on Mullite and BSAS, *J. Am. Ceram. Soc.*, 86(8), 2003, 1299–1306.

[6] K. Lee, D. Fox, N. Bansal, Rare Earth Silicate Environmental Barrier Coatings for SiC/SiC Composites and Si₃N₄ Ceramics, *Journal of the European Ceramic Society*, Volume 25, Issue 10, 2005, 1705-1715

[7] E. Opila, R. Hann, Paralineer Oxidation of CVD SiC in Water Vapor, *J. Am. Ceram. Soc.*, 80(1), 1997, 197-205.

[8] E. Opila, Variation of the Oxidation Rate of Silicon Carbide with Water-Vapor Pressure, *J. Am. Ceram. Soc.*, 82(3), 1999, 625-636.

[9] B. Harder, M. Presby, J. Salem. S. Arnold, S. Mital, Environmental Barrier Coating Thermal Oxidation and Adhesion Strength, *ASME J. Eng. Gas Turbines Power*, (143), 2021.

[10] R. Bhatt, S. Choi, L. Cosgriff, D. Fox, K. Lee, Impact Resistance of EBC Coated SiC/SiC CMCs, *J. of Matl. Sci. & Eng.*, 2008, 8-19.

[11] S. Choi, Foreign Object Damage in CMCs, *Ceramic Matrix Composites* (1), 2015, 405-429.

[12] S. Choi, J. Wright, C. Faucett, M. Ayre, Phenomena of Foreign Object Damage by Spherical Projectiles in EB-PVD Thermal Barrier Coatings of Turbine Airfoils, *ASME J. Eng. Gas Turbines Power*, (136), 2014.

[13] N. Kedir, E. Garcia, C. Kirk et. al., In-situ characterization of foreign object damage in environmental barrier coated silicon carbide, *J. Am. Ceram. Soc.*, 2020, 1-16.

[14] S. Choi, Z. Racz, Effects of Target Size on Foreign Object Damage in Gas-Turbine Grade Silicon Nitrides by Steel Ball Projectiles, *ASME J. Eng. Gas Turbines Power*, (134), 2012.

[15] M. Presby, R. Mansour, M. Kannan et. al., Characterization and simulation of foreign object damage in curved and flat SiC/SiC ceramic matrix composites, *Ceram. Int.* (45), 2019, 2635-2643.

[16] K. Kane, E. Garcia et. al., Steam oxidation of ytterbium disilicate environmental barrier coatings with and without a silicon bond coat. *J. Am. Ceram. Soc.* (104), 2021. 2285-2300.

[17] K. Lee, A. Garg, W. Jennings, Effects of the Chemistry of Coating and Substrate on the Steam Oxidation Kinetics of Environmental Barrier Coatings for Ceramic Matrix Composites, *J. Eur. Ceram. Soc.* (41), 2021, 5675-5685.

[18] K. Lee, D. Waters, B. Puleo, A. Garg, W. Jennings, G. Costa, D. Sacksteder, Development of Oxide-based High Temperature Environmental Barrier Coatings for Ceramic Matrix Composites via the Slurry Process, *J. Eur. Ceram. Soc.* (41), 2021, 1639-1653.

[19] N. Kedir, E. Garcia, C. Kirk et. al., Impact damage of narrow silicon carbide (SiC) ceramics with and without environmental barrier coatings (EBCs) by various foreign object debris (FOD) simulants, *Surface Coatings and Tech.* (407), 2021.

[20] K. Lee, $\text{Yb}_2\text{Si}_2\text{O}_7$ EBCs with Reduced Bond Coat Oxidation Rates Via Chemical Modifications for Long Life, *J. Am. Ceram. Soc.* (102), 2019, 1507-1521.

[21] J. Salem, S. Mital, B. Harder, A. Thompson, Design of an Environmental Barrier Coating Bond Strength Test Coupon, *Proc. ASME Turbo Expo*, 2023.

[22] ASTM, 2015, Standard Test Method for Through-Thickness “Flatwise,” Tensile Strength and Elastic Modulus of a Fiber-Reinforced Polymer Matrix Composite Material, West Conshohocken, PA, Standard No. ASTM D7291/D7291M-15.